International Journal of Mechanical Sciences 133 (2017) 376–386

Contents lists available at ScienceDirect

International Journal of Mechanical Sciences

journal homepage: www.elsevier.com/locate/ijmecsci

Free vibration analysis of cylindrical panels with spiral cross section

A. Taraghi Osguei [a,b], M.T. Ahmadian [a,c,*], M. Asghari [a], N.M. Pugno [b,d,e]

[a] Department of Mechanical Engineering, Sharif University of Technology, Tehran, Iran
[b] Laboratory of Bio-Inspired and Graphene Nanomechanics, Department of Civil, Environmental and Mechanical Engineering, University of Trento, Trento, Italy
[c] Center of Excellence in Design, Robotics and Automation (CEDRA), Sharif University of Technology, Tehran, Iran
[d] School of Engineering and Material Science, Queen Mary University of London, London, UK
[e] Ket Lab, Edoardo Amaldi Foundation, Italian Space Agency, Via del Politecnico snc, 00133 Rome, Italy

ARTICLE INFO

Keywords:
Thin shell
Free vibration
Noncircular cylinder
Spiral cross section
Rayleigh-Ritz technique

ABSTRACT

In this paper, free vibration of open noncircular cylinders with spiral cross section are studied under arbitrary boundary conditions. For deriving the strain energy function, Kirchhoff-Love hypotheses are employed. To obtain the solutions, Rayleigh-Ritz technique is implemented by selecting Chebyshev orthogonal polynomials of first kind as admissible displacement functions in three directions. Convergence of the proposed formulation is verified for spiral cylindrical panel and the results are compared with those of ABAQUS. Parametric study is undertaken to highlight the effect of inner radius, separation distance, subtended angle, thickness, and length of the spiral cylinders on the free vibration characteristics. Results obtained in this research are the first step toward modeling spiral cylinders and can be used for comparison in future studies. Finally, the design strategy for the spiral cylinders with specific vibration characteristics is presented. The results imply that spiral cylinder with specific vibration characteristics can be designed using equivalent open circular cylinder.

1. Introduction

Research on the vibration of cylindrical shells is not a new topic and the first reference dates 1970s [1]. Shells are one of the most useful elements in industry and civil to construct complicated Structures. These structures vary from roof of a building to wing of a flight. Their application in different fields requires precise analysis of the static and dynamic behavior considering design and safety issues.

Cylindrical shells are one of the most principal elements used in engineering structures and the vibration behavior of them is an interesting topic for researchers even after decades [2–5]. Numerous studies on closed circular cylinders cover different aspects of their vibration behavior [6–8]. The effect of variable thickness of closed circular cylinder, in axial and circumferential directions, on vibration of shell has been studied [9,10]. Different boundary conditions and vibration behavior of composite cylinders are other interesting topics for researcher [11–14]. Meanwhile, similar studies have been carried out on open circular shells [15–19].

Noncircular cylinders have been studied as closed shells and open panels in two different categories like circular cylinders [20]. Suzuki et al. investigated the vibration characteristics of closed noncircular thin and thick shells [21,22]. Most of the researches on closed noncircular cylinders are focused on special cross sections such as oval [23] and elliptic profiles [24–26]. Although some of researchers have investigated the closed noncircular cylindrical shells with arbitrary cross section, they have treated oval and elliptic shells as examples.

Soldatos reviewed the studies on mechanics of cylindrical shells with noncircular cross section including vibration characteristics [27]. As clarified in the survey, due to difficulties of open noncircular panels comparing with circumferentially closed cylindrical shells, the research on the open noncircular cylindrical panels have received little attention. Srinivasan and Bobby studied the vibration characteristics of oval panels by considering all edges of panel are clamped and investigated the effect of parameters such as curvature, thickness and aspect ratio [28]. Massalas et al. used Donnell's theory to study the natural frequencies of noncircular shells with arbitrary boundary conditions and applied this method on oval shells in special boundary conditions [29]. Koumousis and Armenakas investigated free vibration of noncircular cylindrical panels with simply supported curved edges using Flugge and Donnell type equations and applied the method on symmetric panels [30]. In addition, Koumousis and Armenakas analyzed the free vibration of oval cylindrical panels with simply supported curved edges [31]. Suzuki et al. developed and exact solution procedure for determining the natural frequencies of open noncircular shells supported by shear diaphragm in curved edges and the method was applied for shells having elliptical cylindrical curvature and circumferentially varying thickness [32].

* Corresponding author at: Department of Mechanical Engineering, Sharif University of Technology, Tehran, Iran.
E-mail address: ahmadian@sharif.edu (M.T. Ahmadian).

http://dx.doi.org/10.1016/j.ijmecsci.2017.07.044
Received 21 November 2016; Received in revised form 7 July 2017; Accepted 19 July 2017
Available online 12 August 2017
0020-7403/

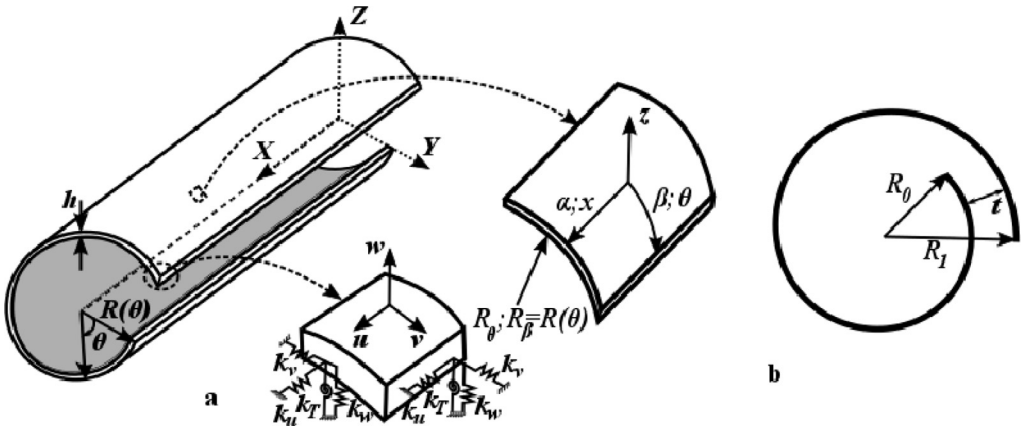

Fig. 1. Geometry of a cylindrical panel with spiral cross section (a) cylindrical panel (b) spiral cross section of mid-surface.

Koumousis presented a new method for obtaining the dynamic characteristics of cylindrical panels with noncircular cross section having simply supported curved edges using Flugge and Donnell type equations [33]. The researcher claimed that mentioned method is efficient in determining the eigenfrequencies and corresponding mode shapes. Grigorenko et al. investigated free vibration of elastic isotropic open cylindrical shell with elliptic cross section using spline-collocation method [34].

There are rare publications on the vibration of open noncircular shells comparing with the circular ones in the literature. Additionally, these studies on noncircular shells are concentrated on oval and elliptic cross sections. In this paper, free vibration of a cylindrical panel with spiral cross section as an open noncircular shell is studied. Spiral cross section is a well-known configuration in some general structures like large span roofs [35] and specific applications like carbon nanoscrolls [36–39]. In addition, spiral cylinders can be the result of imperfection in production process of circular cylindrical panels.

Although some of pervious researches studied open noncircular shell as an arbitrary profile, they are usually limited to Flugge and Donnell's theory with special boundary conditions on the edges of panel [33]. In the present research, with no limitation on the boundary conditions, any classical and non-classical constrains can be applied along the straight and curved edges of the panel for analyzing vibration characteristics of spiral cylinders. In this study, displacement functions of the shell in each direction are expanded as Chebyshev polynomials of first kind. After convergence analysis, results are compared with finite element model using ABAQUS commercial software.

2. Modeling

Fig 1 shows an open noncircular cylindrical shell with length, L, circumferential subtended angle, ϕ, and linearly varying radius. The cylindrical coordinate system ($x\ \theta\ z$) illustrated on the shell segment might be used for describing the equations of motion. u, v, and w denote the displacement components in these directions, respectively. The radius of curvature in circumferential direction of mid-surface is R_θ. The global Cartesian coordinate system (XYZ) would be used to describe the position vector of a typical point on mid-surface of shell. The translational springs (k_u,k_v,k_w) and torsional spring (k_T) are uniformly distributed along the boundaries to model the resultant forces in each boundary. The inner and outer radii of the cross section are R_0 and R_1, respectively. The term t shows the distance between two successive turns of spiral which is called separation distance and the thickness of shell is assumed to be h.

The position of a typical point in the mid-surface of a cylindrical shell with Archimedean spiral cross section can be defined in terms of x and θ as:

$$\vec{r}(x,\theta) = x\,\hat{I} + (R_0 + a\theta)\cos\theta\,\hat{J} + (R_0 + a\theta)\sin\theta\,\hat{K} \tag{1}$$

where $\hat{I}$, $\hat{J}$, and $\hat{K}$ denote the unit vectors along X, Y, and Z. Parameter a which controls the distance between two successive turns of spiral equals $t/2\pi$. By considering the ratio a/R_0 to be small and using formulation presented in Appendix A, the Lame parameters for the cylindrical panel with spiral cross section could be described as:

$$A = 1 \tag{2.a}$$

$$B = \sqrt{a^2 + (R_0 + a\theta)^2} \approx R_0 + a\theta \tag{2.b}$$

and the curvature radii of the shell along two directions can be determined by:

$$R_x = \infty \tag{3.a}$$

$$R_\theta = \frac{\sqrt{(a^2 + (R_0 + a\theta)^2)^3}}{2a^2 + (R_0 + a\theta)^2} \approx R_0 + a\theta \tag{3.b}$$

By considering linear variation of in-plane displacements through the thickness of the shell and satisfying the Kirchhoff-Love assumptions, the components of strain in an arbitrary point of a shell are commonly expressed by separating membrane and bending strains as:

$$\begin{aligned} \varepsilon_{xx} &= \varepsilon^0_{xx} + z\,k_{xx} \\ \varepsilon_{\theta\theta} &= \varepsilon^0_{\theta\theta} + z\,k_{\theta\theta} \\ \gamma_{x\theta} &= \gamma^0_{x\theta} + z\,k_{x\theta} \end{aligned} \tag{4}$$

in which ε^0_{xx}, $\varepsilon^0_{\theta\theta}$, and $\gamma^0_{x\theta}$ are normal and shear strains independent of z direction. k_{xx}, $k_{\theta\theta}$, and $k_{x\theta}$ represent variation of curvatures and twist in mid-surface, respectively. Considering the geometric parameters of a spiral cylindrical panel, described in relations (1)–(3), and using Kirchhoff-Love assumptions, the strain-displacement relations of mid-surface are:

$$\begin{aligned} \varepsilon^0_{xx} &= \frac{\partial u}{\partial x};\ \varepsilon^0_{\theta\theta} = \frac{1}{R_0 + a\theta}\frac{\partial v}{\partial \theta} + \frac{w}{R_\theta} \\ \gamma^0_{x\theta} &= \frac{\partial v}{\partial x} + \frac{1}{R_0 + a\theta}\frac{\partial u}{\partial \theta};\ k_{xx} = -\frac{\partial^2 w}{\partial x^2} \\ k_{\theta\theta} &= \frac{1}{(R_0 + a\theta)^2}\frac{\partial v}{\partial \theta} - \frac{1}{(R_0 + a\theta)^3}\frac{\partial R_\theta}{\partial \theta}v \\ &\quad + \frac{1}{(R_0 + a\theta)^3}\frac{\partial B}{\partial \theta}\frac{\partial w}{\partial \theta} - \frac{1}{(R_0 + a\theta)^2}\frac{\partial^2 w}{\partial \theta^2} \\ k_{x\theta} &= \frac{1}{R_0 + a\theta}\frac{\partial v}{\partial x} - \frac{2}{R_0 + a\theta}\frac{\partial^2 w}{\partial x \partial \theta} \end{aligned} \tag{5}$$

Generalized Hook's law determines the components of stress in each point of the shell according to strain components calculated through

relations (4) and (5):

$$\sigma_{xx} = \frac{E}{1-\nu^2}\epsilon_{xx} + \frac{\nu E}{1-\nu^2}\epsilon_{\theta\theta}$$
$$\sigma_{\theta\theta} = \frac{\nu E}{1-\nu^2}\epsilon_{xx} + \frac{E}{1-\nu^2}\epsilon_{\theta\theta}$$
$$\tau_{x\theta} = \frac{E}{2(1+\nu)}\gamma_{x\theta} \tag{6}$$

where,σ_{xx}, $\sigma_{\theta\theta}$, and $\tau_{x\theta}$ represent normal stresses and shear stress, respectively. E is Young Modulus and ν shows Poison ratio of open cylindrical shell. Force and moment applied on the panel can be calculated by integrating components of stress along the thickness of shell:

$$N_{xx} = \frac{E\,h}{1-\nu^2}\epsilon^0_{xx} + \frac{\nu\,E\,h}{1-\nu^2}\epsilon^0_{\theta\theta}$$
$$N_{\theta\theta} = \frac{\nu\,E\,h}{1-\nu^2}\epsilon^0_{xx} + \frac{E\,h}{1-\nu^2}\epsilon^0_{\theta\theta}$$
$$N_{x\theta} = \frac{E\,h}{2(1+\nu)}\gamma^0_{x\theta} \tag{7a}$$

$$M_{xx} = \frac{E\,h^3}{12(1-\nu^2)}k_{xx} + \frac{\nu\,E\,h^3}{12(1-\nu^2)}k_{\theta\theta}$$
$$M_{\theta\theta} = \frac{\nu\,E\,h^3}{12(1-\nu^2)}k_{xx} + \frac{E\,h^3}{12(1-\nu^2)}k_{\theta\theta}$$
$$M_{x\theta} = \frac{E\,h^3}{24(1+\nu)}k_{x\theta} \tag{7b}$$

Using relations (5) and (7) one can write the total strain energy of the deformation stored in the spiral cylindrical panel as:

$$U = \iint_S \frac{1}{2}(N_{xx}\epsilon^0_{xx} + N_{\theta\theta}\epsilon^0_{\theta\theta} + N_{x\theta}\epsilon^0_{x\theta} + M_{xx}k_{xx} + M_{\theta\theta}k_{\theta\theta} + M_{x\theta}k_{x\theta})ds \tag{8}$$

The corresponding kinetic energy of the shell can be written as:

$$T = \iint_S \frac{\rho h}{2}\left(\left(\frac{\partial u}{\partial t}\right)^2 + \left(\frac{\partial v}{\partial t}\right)^2 + \left(\frac{\partial w}{\partial t}\right)^2\right)ds \tag{9}$$

where ρ denotes the mass density of the shell and t represents time parameter. The energy stored in the boundary springs which simulates the boundary conditions effect is other component of energy. This energy could be calculated as following:

$$\begin{aligned} U_b = &\int_0^{\phi}\left[k_u^{x_0}u^2 + k_v^{x_0}v^2 + k_w^{x_0}w^2 + k_T^{x_0}\left(\frac{\partial w}{\partial x}\right)^2\right]_{x=0}(R_0 + a\theta)d\theta \\ &+ \int_0^{\phi}\left[k_u^{x_L}u^2 + k_v^{x_L}v^2 + k_w^{x_L}w^2 + k_T^{x_L}\left(\frac{\partial w}{\partial x}\right)^2\right]_{x=L}(R_0 + a\theta)d\theta \\ &+ \int_0^{L}\left[k_u^{\theta_0}u^2 + k_v^{\theta_0}v^2 + k_w^{\theta_0}w^2 + k_T^{\theta_0}\left(\frac{\partial w}{\partial x}\right)^2\right]_{\theta=0}dx \\ &+ \int_0^{L}\left[k_u^{\theta_\phi}u^2 + k_v^{\theta_\phi}v^2 + k_w^{\theta_\phi}w^2 + k_T^{\theta_\phi}\left(\frac{\partial w}{\partial x}\right)^2\right]_{\theta=\phi}dx \end{aligned} \tag{10}$$

in which $k_i^{j_s}$ $i = u, v, w, T$; $j_s = x_0, x_L, \theta_0, \theta_\phi$ represent the stiffness of springs located at boundary edge j_s in different directions. For example, $k_w^{x_0}$ shows the stiffness of spring in z direction located at boundary $x = 0$. Using the energy components calculated through relations (8)–(10), total Lagrangian energy functional for a noncircular cylindrical panel with spiral cross section and arbitrary boundary condition in straight and curved edges could be written:

$$L = T - U - U_b \tag{11}$$

In this study, Rayleigh- Ritz method is used to determine the natural frequencies and mode shapes of the panel. Effect of boundary conditions are embedded in energy function, consequently, any independent and complete bases functions can be considered as admissible functions and they are not needed to satisfy any boundary condition. Therefore, Chebyshev polynomials of first kind are considered as admissible functions for displacement components in three directions:

$$u(x,\theta,t) = \sum_{m=0}^{\infty}\sum_{n=0}^{\infty}U_{mn}P_m(x)P_n(\theta)e^{j\omega t}$$
$$v(x,\theta,t) = \sum_{m=0}^{\infty}\sum_{n=0}^{\infty}V_{mn}P_m(x)P_n(\theta)e^{j\omega t}$$
$$w(x,\theta,t) = \sum_{m=0}^{\infty}\sum_{n=0}^{\infty}W_{mn}P_m(x)P_n(\theta)e^{j\omega t} \tag{12}$$

where, U_{mn}, V_{mn}, and W_{mn} are unknown coefficients of displacement functions. $P_m(x)$, and $P_n(\theta)$ represent Chebyshev polynomials of first kind as following:

$$P_0(s) = 1;\quad P_1(s) = s$$
$$P_i(s) = 2sP_{i-1}(s) - P_{i-2}(s)\quad i > 1 \tag{13}$$

Chebyshev polynomials of first kind are defined on the interval [−1, 1]. Therefore, the length of the cylinder should be transformed to this interval. A coordinate transformation between the dimensions of cylinder and mentioned interval, $\bar{x} = 2x/L - 1$; $\bar{\theta} = 2\theta/\phi - 1$, is needed.

Due to limitations of calculation, the series expansion should be truncated. Therefore, proper precision can be achieved by the selection of M and N as the summation limits. Substituting relation (12) into Eqs. (8)–(11) and minimizing total Lagrangian energy with respect to unknown coefficients of displacement, leads to the following eigenvalue problem.

$$\left(\begin{bmatrix} K_{uu} & K_{uv} & K_{uw} \\ K_{vu} & K_{vv} & K_{vw} \\ K_{wu} & K_{wv} & K_{ww} \end{bmatrix} - \omega^2\begin{bmatrix} M_{uu} & 0 & 0 \\ 0 & M_{uu} & 0 \\ 0 & 0 & M_{uu} \end{bmatrix}\right)\begin{Bmatrix} U \\ V \\ W \end{Bmatrix} = 0 \tag{14}$$

Where K_{ij} and M_{ij}; $i, j = u, v, w$ denote sub-matrices of generalized stiffness and generalized mass matrices which their elements are represented in Appendix B. The vectors U, V, and W are undetermined coefficients of displacement which construct the corresponding mode shapes of each natural frequency:

$$U^T = [U_{00}, \ldots, U_{0N}, U_{10}, \ldots, U_{1N}, \ldots, U_{M0}, \ldots, U_{MN}]$$
$$V^T = [V_{00}, \ldots, V_{0N}, V_{10}, \ldots, V_{1N}, \ldots, V_{M0}, \ldots, V_{MN}]$$
$$W^T = [W_{00}, \ldots, W_{0N}, W_{10}, \ldots, W_{1N}, \ldots, W_{M0}, \ldots, W_{MN}] \tag{15}$$

One can obtain the natural frequencies of noncircular shell with spiral cross section by solving the standard eigenvalue problem. Substituting corresponding eigenvector of each natural frequency to displacement relations gives the mode shapes.

3. Results and discussion

In order to study the effect of geometric parameters of spiral cylindrical panel on the vibration characteristics, a computer program has been developed. Although there is no limitation on the application of any boundary condition, reporting the results of every combination of boundary conditions is impossible. In this research, one of the main goals is selecting appropriate geometrical parameters of a spiral cylindrical panel to achieve desired vibration behavior. Therefore, in most of the simulations, all edges of the panel are considered to be free. In this investigation, simply support boundary condition beside the free boundary condition is interested to serve suitable results for future studies. In addition, some results are reported for completely clamped and completely supported by shear diaphragm boundary conditions in all edges of spiral panel.

Defining the stiffness of springs uniformly distributed along each edge of the panel depends on the boundary conditions. Based on the

Table 1
Convergence of first seven natural frequencies for completely free cylindrical panel with spiral cross section ($R_0 = 2m,\ t = 1m,\ \phi = 2\pi,\ L = 5m,\ h = 0.1m$).

Mode Shape	M=N							ABAQUS
	4	8	11	12	13	14	15	
1	4.36	1.75	1.74	1.75	1.75	1.75	1.75	1.74
2	4.58	2.32	2.47	2.32	2.32	2.32	2.32	2.47
3	11.75	3.89	3.80	3.82	3.82	3.82	3.82	3.80
4	12.35	5.34	5.34	5.30	5.30	5.30	5.30	5.34
5	104.00	9.31	8.50	8.54	8.54	8.54	8.54	8.49
6	168.28	9.94	9.21	9.61	9.60	9.60	9.60	9.20
7	175.63	18.29	15.02	15.78	15.78	15.78	15.78	15.00

analysis presented in Section 3.1, the boundary spring rigidities can be expressed for classical boundary conditions including free, simply support, clamped, and shear diaphragm on the curved edge $x = 0$ as an example:

Free (F): $k_u^{x_0} = 0, k_v^{x_0} = 0, k_w^{x_0} = 0, k_T^{x_0} = 0$
Simply Support (S): $k_u^{x_0} = 10^9 D, k_v^{x_0} = 10^9 D, k_w^{x_0} = 10^9 D, k_T^{x_0} = 0$
Clamped (C): $k_u^{x_0} = 10^9 D, k_v^{x_0} = 10^9 D, k_w^{x_0} = 10^9 D, k_T^{x_0} = 10^9 D$
Shear Diaphragm (D): $k_u^{x_0} = 0, k_v^{x_0} = 10^9 D, k_w^{x_0} = 10^9 D, k_T^{x_0} = 0$

where $D = Eh^3/12(1-\nu^2)$ is bending stiffness of the panel. Since there are four edges for an open cylindrical panel, a simple letter string like FSCD is employed to represent the boundary conditions of the spiral cylinder. FSCD indicates a spiral cylinder with free, simply support, clamped, shear diaphragm boundary conditions at the edges $x = 0$, $x = L$, $\theta = 0$, and $\theta = \phi$, respectively.

3.1. Convergence and accuracy

The first crucial step to use the proposed method in vibration analysis of spiral cylinder is determination of truncation number for displacement series expansion. Although the values of M and N depend on the geometric properties of panel, boundary conditions, mode number, and the accuracy of results, usually there is a constant value for specific structure. In the convergence study, the natural frequencies of a completely free spiral cylinder with different truncation numbers are presented. Table 1 demonstrates first seven natural frequencies of a spiral cylinder with following geometric parameters: $R_0 = 2m,\ t = 1\ m,\ \phi = 2\pi,\ L = 5\ m$, and $h = 0.1$ m. For all numerical results in this research, unless otherwise stated, the material properties are $E = 210$ GPa, $\rho = 7800\ \text{kg/m}^3$, $\nu = 0.3$. The results show that the natural frequencies converge quickly. Verification of the formulation in this study could be achieved by comparison between the results of the proposed method and those obtained through ABAQUS. The geometric profile of the spiral cross section is created in ABAQUS through the Python script and 3465 uniform shell elements are used for simulation. The applied elements are four-node doubly curved thin or thick shell elements (S4R) of ABAQUS standard element library.

The previous researchers usually studied the circular cylinders and researches on noncircular cylindrical panels are limited to oval and elliptic ones. Considering the lack of results on the vibration characteristics of spiral cylinders in the literature, a possible strategy for verification of results and comparing with the literature can be achieved by simplifying the formulation of a noncircular spiral cylinder into a circular cylinder and comparing with previous studies. Therefore, by putting separation distance, t, equal to zero a circular cylinder is modeled as: $R_0 = 2\ m$, $t = 0$, $\phi = \pi/2$, $L = 3\ m$, and $h = 0.02$ m. The first four frequency parameters, $\Omega = 2\pi\omega R\sqrt{\rho/E}$, of the cylinder are given in Table 2 and corresponding mode shapes are shown in Fig 2. However, more verification of the presented method on circular cylindrical, spherical, and conical panels could be found in Refs. [18,40,41].

If the separation distance of a cylindrical panel is not zero, the comparison of results with literature is impossible and the results obtained by proposed method can be compared with those of ABAQUS software. Therefore, two cylindrical panels with spiral cross sections are modeled as: Example 1 ($R_0 = 3\ m,\ t = 1\ m,\ \phi = \pi,\ L = 5\ m$, and $h = 0.01$ m), Example 2 ($R_0 = 4\ m,\ t = 1.5\ m,\ \phi = 5\pi/2,\ L = 30\ m$, and $h = 0.01$ m). The boundary conditions FCCC and FCFC are considered for Example 1 and Example 2, respectively. The first four natural frequencies of these cylinders are determined and reported in Table 3 and the corresponding mode shapes are illustrated in Figs 3 and 4 using proposed method and ABAQUS model. For the ABAQUS simulation, the model contains 5100 and 14,550 shell elements for Example 1 and Example 2, respectively.

Table 2
Comparison of first four frequency parameters for FCCC cylindrical panel with circular cross section ($R_0 = 2m,\ t = 0,\ \phi = \pi/2,\ L = 3m,\ h = 0.02m$).

Mode shape	Present	Ref. [18]
1	0.1529	0.1529
2	0.1787	0.1787
3	0.2819	0.2819
4	0.2877	0.2877

Table 3
First four frequency parameters for Examples 1 and 2 determined through proposed method and ABAQUS software.

	Example 1		Example 2	
Mode shape	Present	ABAQUS	Present	ABAQUS
1	0.0514	0.0516	0.0027	0.0027
2	0.0517	0.0519	0.0070	0.0070
3	0.0644	0.0648	0.0076	0.0076
4	0.0673	0.0677	0.0084	0.0085

The effect of boundary springs rigidity on the natural frequency is studied to check the appropriateness of boundary conditions modeling. Fig 5 shows the frequency parameter, $\Omega = \omega L^2\sqrt{\rho h/D}$, versus different elastic restraint parameter in one of the boundaries. A spiral cylinder with $R_0 = 2\ m,\ t = 1\ m,\ L = 3\ m$, and $h = 0.05$ m by two subtended angles $\phi = \pi/3$ and $\phi = \pi$ is studied and the results compared with circular cylinder by putting separation distance equal to 0. When three springs stiffness of a boundary condition is zero and elastically restrained in one direction the boundary could be defined as E_I. Consequently, when the three groups of the springs get infinite stiffness, 10^9D, the boundary could be represented with E_{II}.

Fig 5(a) and (b) show the variation of first frequency parameter in CE_IFF and $CE_{II}FF$ boundary conditions for spiral and circular cylinders when subtended angle equals to $\phi = \pi/3$. The results for a bigger subtended angle, $\phi = \pi$, in Fig 5(c) and (d) reveal the effect of cross section in natural frequencies.

3.2. Parameter study

From design perspective, it is important to know the influence of each parameter on the vibration characteristics of the panel. In this

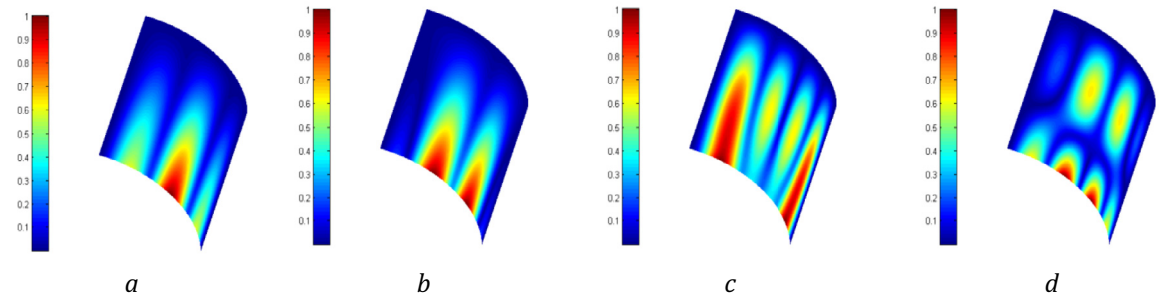

Fig. 2. First four mode shapes of FCCC cylindrical panel with circular cross section.

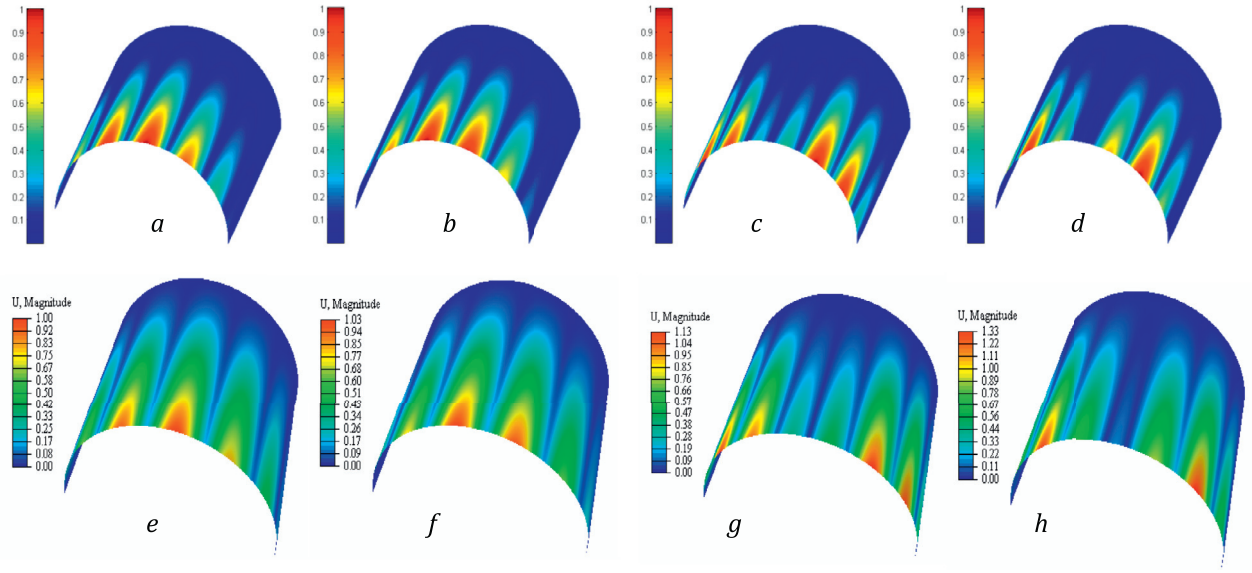

Fig. 3. First four mode shapes of Example 1 calculated through the proposed method (a-d) and ABAQUS (e-h).

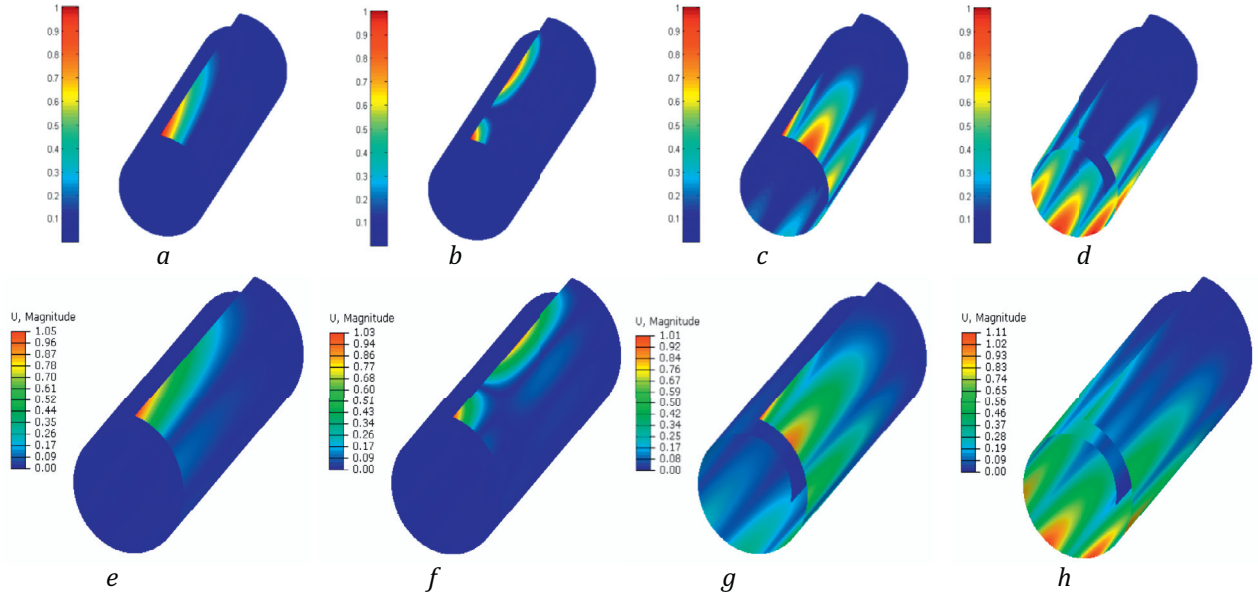

Fig. 4. First four mode shapes of Example 2 calculated through the proposed method (a-d) and ABAQUS (e-h).

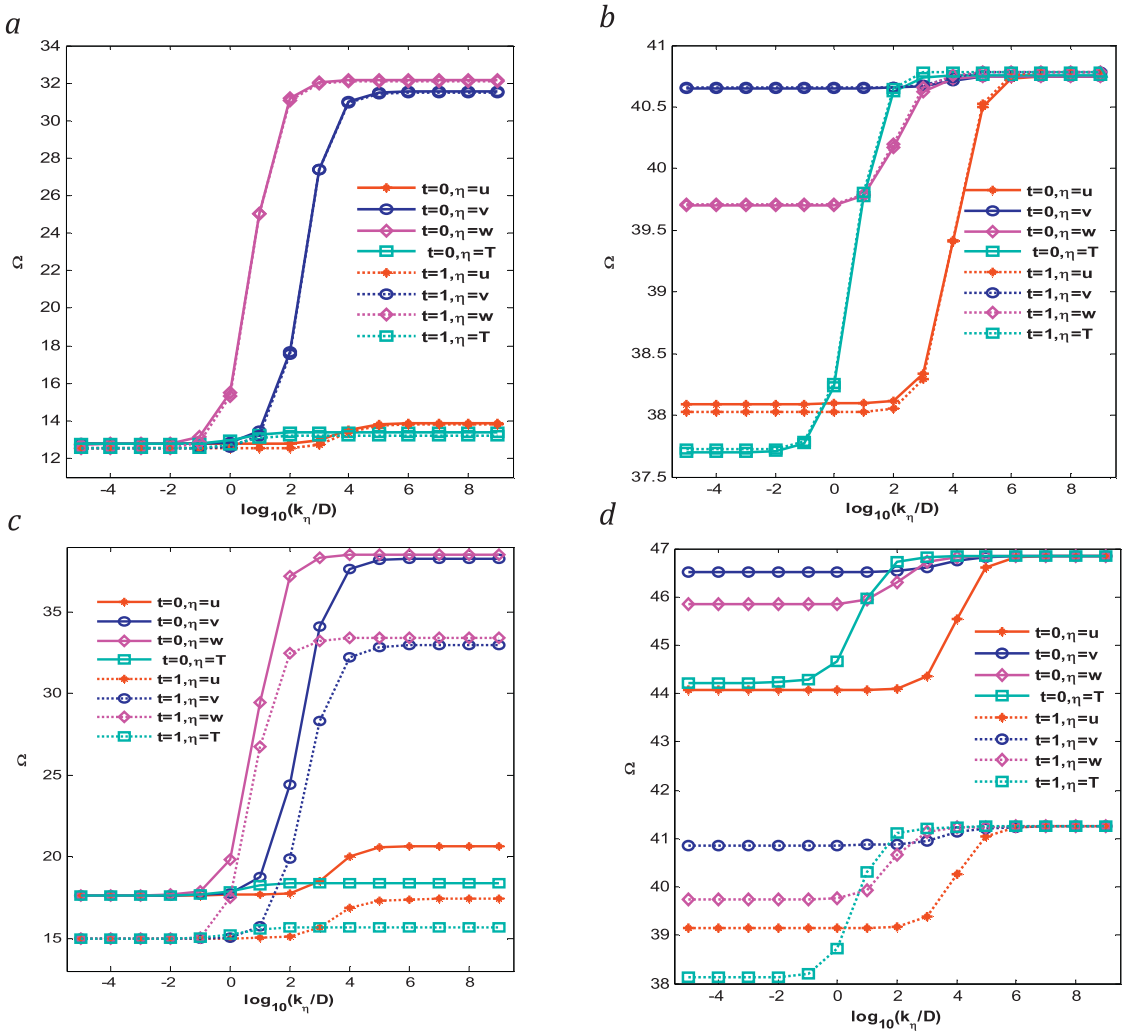

Fig. 5. Variation of first frequency parameter for spiral cylinder with two different subtended angles for elastic boundary conditions (a) $\phi=\pi/3$, CE_IFF (b) $\phi=\pi/3$ $CE_{II}FF$ (c) $\phi=\pi$, CE_IFF (d) $\phi=\pi$ $CE_{II}FF$.

section, the effect of each geometric parameter in natural frequency and corresponding mode shape is studied by considering the other parameters are constant. Table 4 represents the lowest four natural frequencies of the spiral cylinder with different classical boundary conditions to investigate the frequency change with respect to variation of separation distance.

When separation distance increases the cylinder degenerates from a circular to spiral cylinder. According to formulation, ratio of separation distance to radius should be small. However, comparison of the results obtained by proposed method and ABAQUS demonstrate high accuracy of the proposed formulation even for $t/R_0=1$.

Generally, separation distance shows a decreasing effect on the natural frequencies of spiral cylindrical panel and it is more considerable in FFFF boundary condition comparing with other boundary conditions. However, the first natural frequency shows an opposite behavior for FFSS boundary condition and corresponding mode shape is a special mode which appears only in this boundary condition. Restricting straight edges by simply support shows more effect on natural frequencies than restriction on curved edges. Meanwhile, results for completely clamped and shear diaphragm boundary condition are reported.

In Table 5, a set of examples are conducted to illustrate the influence of inner radius on the vibration behavior of spiral cylinder with different boundary conditions. Although like separation distance, the decreasing influence of inner radius on natural frequency in completely free boundary condition is dominant, the first natural frequency in FFSS boundary condition shows different manner. In addition, the first natural frequency obtained in FFSS is lower than that of FFFF. This strange consequence depends on the appearance of a particular mode shape in FFSS boundary condition.

To study the effect of subtended angle on vibration characteristics, variation of the lowest two natural frequencies of the spiral cylinder against subtended angle with FFFF boundary condition is illustrated in Fig 6. The results are achieved using the parameters of previous example with different subtended angles. Additionally, the corresponding first two mode shapes of the spiral cylinder in selected subtended angles are represented to enhance the understanding of vibration behavior. It can be observed from the figure that first natural frequency increases and reaches the crest in $\phi=45^\circ$ and declines while second natural frequency contains three extrema in $\phi=25^\circ$, 45° and 65°. This firstly reported result shows a different behavior with respect to previously results published on open circular cylinders and could be helpful significantly from design perspective.

Fig 7 shows the trend of first two natural frequencies for SSSS restricting condition versus the subtended angle. From the results it is clear that first two natural frequencies have decreasing trend for SSSS boundary condition while for FFFF boundary condition do not. Although the mode shapes corresponding to this boundary condition are entirely different from FFFF, in both of them as subtended angle increase the

Table 4
First four natural frequencies of spiral cylinder with different separation distances and boundary conditions ($R_0 = 2m$, $\phi = 2\pi$, $L = 5\ m$, $h = 0.1$ m).

Separation Distance	Mode Shape	Boundary Conditions									
t (m)		FFFF	SFFF	FFSS	SSFF	FSSS	SSSF	SSFS	SSSS	CCCC	DDDD
0	1	2.72	19.80	0.00	48.47	49.17	48.48	48.48	106.92	112.07	80.94
	2	3.11	20.14	5.59	48.49	50.78	95.32	95.32	107.96	112.19	86.18
	3	5.91	41.62	5.91	95.32	66.22	103.38	103.38	120.69	128.57	88.92
	4	6.89	46.50	15.18	95.32	69.37	107.81	107.81	125.14	128.80	106.29
0.5	1	2.15	18.19	0.10	43.94	46.58	43.94	48.16	99.79	104.67	77.24
	2	2.66	19.77	4.43	48.15	47.26	87.89	94.92	100.84	105.46	80.12
	3	4.68	40.95	4.69	87.89	59.81	95.45	98.70	111.68	117.09	88.39
	4	5.99	42.27	12.00	94.88	63.48	101.06	100.76	114.22	119.95	90.15
1	1	1.75	16.82	0.15	40.50	43.62	40.50	47.83	92.97	98.11	72.54
	2	2.32	19.58	3.61	47.83	44.90	82.30	92.83	94.11	98.71	77.74
	3	3.82	38.37	3.82	82.30	54.47	88.40	93.92	103.75	109.69	80.37
	4	5.30	42.49	9.72	88.38	58.38	94.32	94.46	106.12	110.48	90.79
1.5	1	1.45	15.71	0.18	37.79	41.45	37.79	47.53	86.72	91.98	68.43
	2	2.05	19.41	3.01	47.53	42.11	77.92	86.71	87.98	92.75	73.48
	3	3.18	36.51	3.17	77.92	51.69	82.29	87.92	96.99	102.31	78.42
	4	4.74	40.36	8.04	82.29	52.49	88.21	94.06	99.03	103.88	81.30
2	1	1.22	14.80	0.18	35.59	39.23	35.59	47.23	81.21	86.68	64.76
	2	1.83	19.24	2.56	47.23	39.95	74.39	81.19	82.45	87.26	69.96
	3	2.70	34.73	2.68	74.39	47.58	77.03	82.46	91.11	96.46	74.06
	4	4.29	38.74	6.76	77.03	49.79	82.71	90.62	92.75	97.48	79.47
ABAQUS	1	1.21	14.82	0.18	35.39	39.12	35.39	47.27	81.15	86.48	64.39
	2	1.83	19.43	2.27	47.27	39.87	73.68	81.14	82.40	87.22	69.81
	3	2.65	34.63	2.48	73.68	47.32	76.88	82.40	90.97	96.30	73.68
	4	4.17	38.74	6.61	76.88	49.68	82.65	90.71	92.70	97.29	79.76

Table 5
First four natural frequencies of spiral cylinder with different inner radiuses and boundary conditions ($t = 1\ m$, $\phi = 2\pi$, $L = 5\ m$, $h = 0.1$ m).

Inner Radius	Mode Shape	Boundary Conditions									
R_0 (m)		FFFF	SFFF	FFSS	SSFF	FSSS	SSSF	SSFS	SSSS	CCCC	DDDD
1	1	4.70	20.35	0.74	49.18	56.65	49.18	64.03	120.62	126.43	86.45
	2	4.89	25.62	10.25	64.03	58.09	96.22	118.50	123.55	128.40	95.77
	3	9.91	43.77	10.60	96.22	85.93	110.16	121.49	147.16	156.33	103.80
	4	10.82	50.83	27.09	110.09	87.51	124.22	123.73	153.82	159.63	128.09
2	1	1.75	16.82	0.15	40.50	43.62	40.50	47.83	92.97	98.11	72.54
	2	2.32	19.58	3.61	47.83	44.91	82.30	92.83	94.11	98.71	77.74
	3	3.82	38.37	3.82	82.30	54.47	88.40	93.92	103.75	109.69	80.37
	4	5.30	42.49	9.72	88.38	58.38	94.32	94.46	106.12	110.48	90.79
3	1	0.89	14.70	0.05	35.44	37.07	35.44	39.96	77.58	82.70	63.39
	2	1.40	16.48	1.83	39.96	37.35	74.19	77.51	78.13	83.04	66.24
	3	1.94	33.92	1.95	74.19	43.51	75.10	78.16	83.65	88.67	68.88
	4	3.50	36.01	4.95	75.10	43.82	78.28	81.58	84.25	89.25	71.53
4	1	0.54	13.26	0.03	32.03	32.55	32.03	35.15	67.53	72.81	56.90
	2	0.94	14.53	1.11	35.15	32.76	66.03	67.53	67.86	73.01	56.91
	3	1.17	30.49	1.18	66.02	36.29	67.94	67.83	71.24	76.48	58.92
	4	2.52	32.10	2.99	67.93	37.02	68.75	70.92	71.86	76.82	60.56

first mode shapes contains more waves along the circumferential direction than longitudinal direction. It reflects the fact that cylindrical panels with higher arc length are flexible in circumferential direction and as the arc length decrease the circumferential flexibility diminishes and the first mode shapes contain more waves along the axial direction instead of circumferential direction.

The effect of length and thickness of the shell on the vibration of spiral cylinder is depicted on Figs 8 and 9 with FFFF and SSSS boundary conditions. Generally, in each boundary condition, thickness of the shell has a similar effect on the natural frequency for different length. For example, in Fig 8 the natural frequencies of the shell with thickness 0.1 m is 2.5 times of that in thickness 0.04 m while in SSSS boundary condition in Fig 9 it is 1.5 times bigger than natural frequencies of spiral cylinder with thickness 0.04 m. This diversity could be the result of appearance of bending effect due to boundary condition.

According to the results of Fig 8 first natural frequency in FFFF boundary condition is nearly constant up to length 8 m. However, it shows a decreasing manner for higher values of cylinder length. This variation comes from the mode change which could be observed in mode shapes represented in Fig 8. The natural frequency related to circumferential mode shape, Fig 8(a), has a nearly constant value in different length of cylinder and appears as first and second mode shape by variation of length. In Fig 9, the first and second natural frequencies coincide with each other and as length of cylinder increases the number of waves along the circumferential direction decreases and tends to increase it along the axial direction.

3.3. Design strategy

Since all of the structures and instruments contain mass and elastic properties, they are willing to vibrate. Understanding vibration behavior of engineering elements for safe design of structures and efficient operation of systems is necessary. Structures are usually designed to avoid dangerous failures due to vibration of a specific part. For example, vibration fatigue in components of airplane, gas turbine, and large span roofs is one of the crucial designing criteria. However, vibration in some engineering applications such as actuating elements and casting process

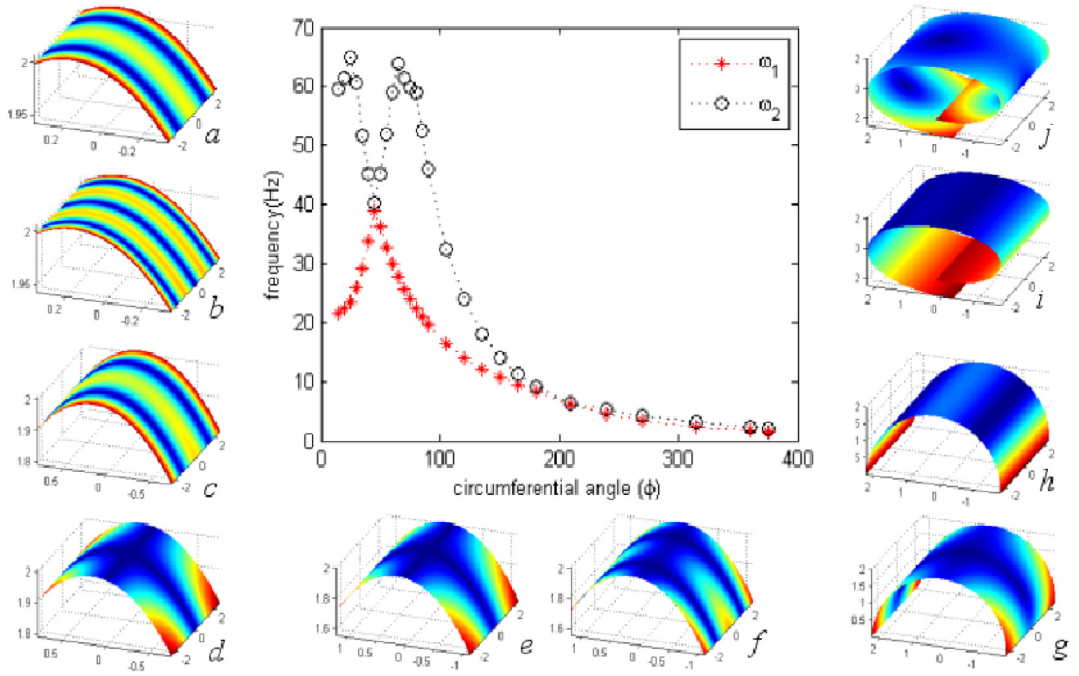

Fig. 6. Variation of natural frequencies versus subtended angle of spiral cylinder and first two mode shapes of selected subtended angles with FFFF boundary condition (a-b) $\phi = 20^{\circ}$, (c-d) $\phi = 45^{\circ}$, (e-f) $\phi = 70^{\circ}$, (g-h) $\phi = 180^{\circ}$, (i-j) $\phi = 375^{\circ}$.

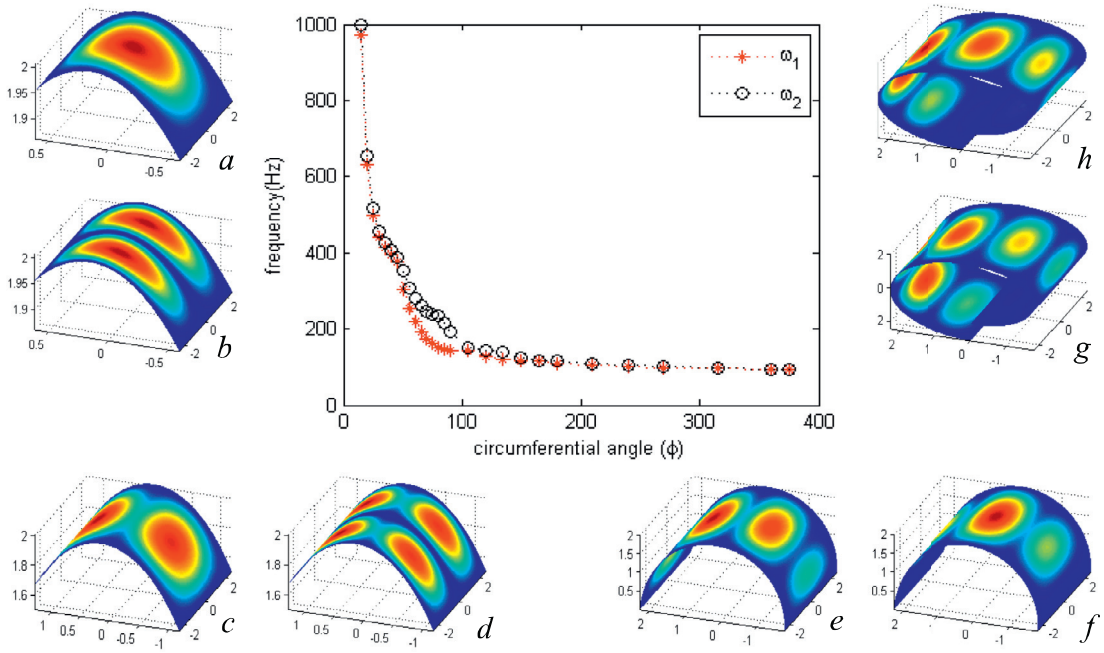

Fig. 7. Variation of natural frequency versus subtended angle of spiral cylinder and first two mode shapes of selected subtended angles with SSSS boundary condition (a-b) $\phi = 35^{\circ}$, (c-d) $\phi = 75^{\circ}$, (e-f) $\phi = 180^{\circ}$, (g-h) $\phi = 360^{\circ}$.

plays a useful role. Therefore, achieving desired vibration performance serves an essential purpose for most of the engineering designs.

The target of this section is proposing a feasible procedure for selecting appropriate geometrical parameters of a spiral cylindrical panel to achieve desired vibration behavior. The geometry of a spiral cylinder can be expressed in terms of inner radius, separation distance, subtended angle, thickness, and length. Based on the results obtained in this study, the non-dimensional parameters, R_{ave}/L, t/L, h/L, and L_θ/L are defined for the sake of generality and convenience. Where $L_\theta = R_{ave}\theta$ represents the arc length of panel and $R_{ave} = R_0 + a\theta/2$ is a new parameter introduced for determining the average radius of a spiral cross section. The non-dimensional natural frequency for expressed variables can be defined as $\Omega = \sqrt{12(1-\upsilon^2)\rho/E}L_\theta\omega$.

Fig 10 shows the variation of frequency parameter for completely free cylindrical panel in selected values of R_{ave}/L and h/L, while Fig 11 presents the effect of separation distance for selected values of R_{ave}/L.

Investigations of this research show that, after introducing R_{ave}/Las a parameter, the effect of separation distance on frequency parameter

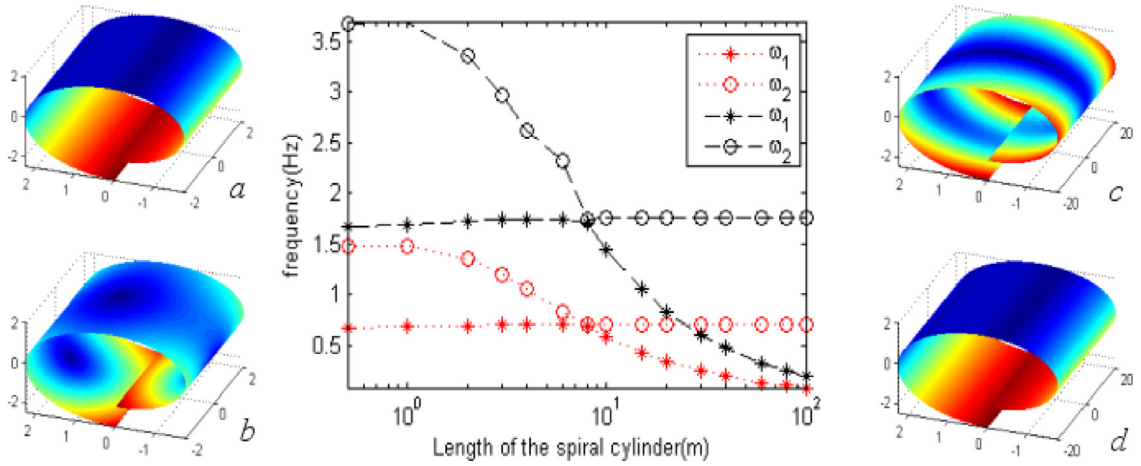

Fig. 8. Variation of natural frequency versus length of spiral cylinder for $h=0.04m$ (…) and $h=0.1m$ (—) and first two mode shapes of selected length with FFFF boundary condition (a-b) $L=4m$, (c-d) $L=40m$.

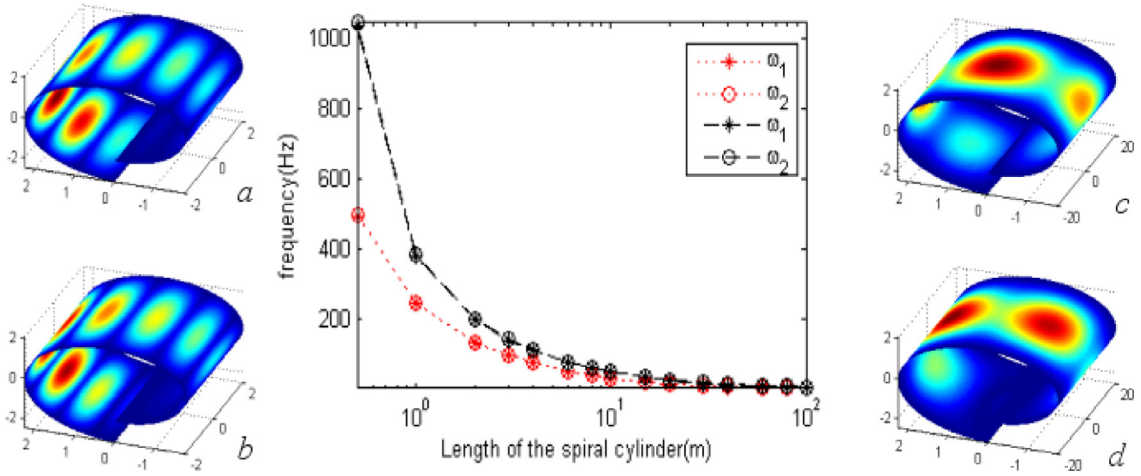

Fig. 9. Variation of natural frequency versus length of spiral cylinder for $h=0.04m$ (…) and $h=0.1m$ (—) and first two mode shapes of selected length with SSSS boundary condition (a-b) $L=4m$, (c-d) $L=40m$.

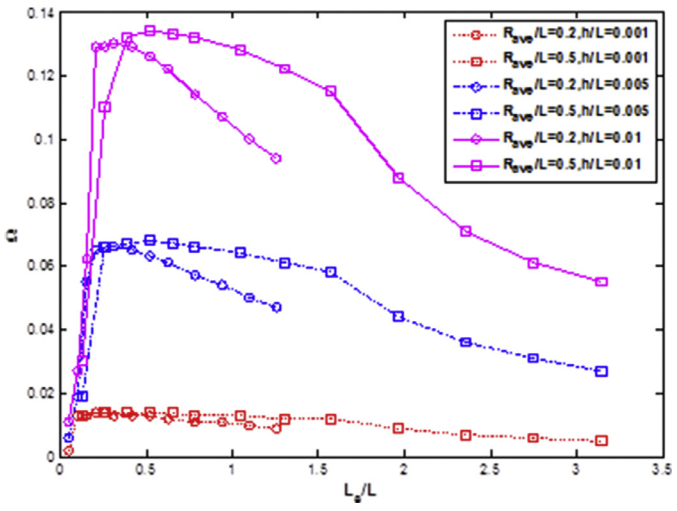

Fig. 10. Variation of first frequency parameter versus ratio of circumferential length to longitudinal length with FFFF boundary condition for selected values of average radius to longitudinal length and thickness to longitudinal length ratios.

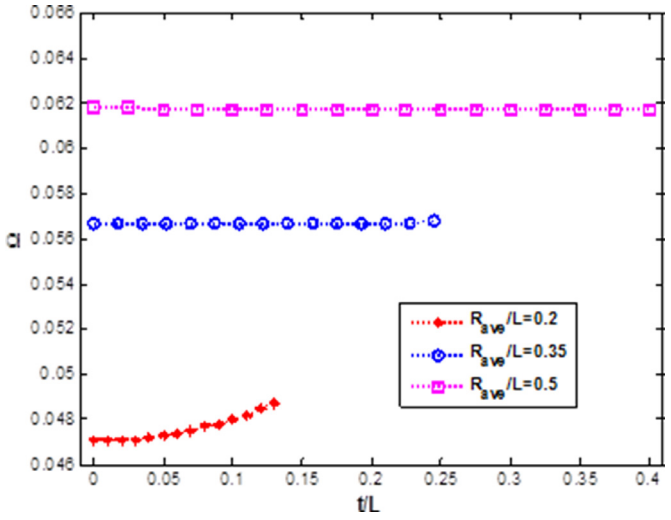

Fig. 11. Variation of frequency parameter versus ratio of separation distance to longitudinal length with FFFF boundary condition for selected values of average radius to longitudinal length ratio in $h/L=0.005$, $L_\theta/L=0.4\pi$.

is small and not comparable with other parameters especially for bigger values of average radius to longitudinal length ratio. However, other parameters including R_{ave}/L, h/L, and L_θ/L are very important in designing process. Therefore, it is appropriate to select parameters of an equivalent circular cylindrical panel at first step by concentrating on the limitations of design to reach the objective predefined natural frequency. In second step, various pairs of separation distance and inner radius can be selected considering average radius defined in pervious step.

4. Conclusion

In this research, a new formulation based on Kirchhoff-Love assumptions is proposed to study the vibration behavior of noncircular cylindrical panels with spiral cross section. The natural frequencies and mode shapes of spiral cylinders are determined through Rayleigh Ritz method. The convergence and accuracy of the results are studied based on the natural frequencies and mode shapes of spiral and circular cylinders. Results obtained from finite element modeling in ABAQUS and previous studies are compared with outcomes of this research and a good agreement is achieved.

The effect of each parameter including inner radius, separation distance, subtended angle, thickness, and length of the spiral cylindrical panel on the vibration characteristics of the shell are investigated through the proposed method. Results indicate that the effect of each parameter on the natural frequencies of the panel varies for different boundary conditions. However, ratio of circumferential length to longitudinal length plays the most important role on natural frequencies and mode shapes of the cylindrical panel. Separation distance as the distinctive characteristic of spiral cylinders, significantly changes the natural frequencies of the panel while other parameters are assumed to be constant. Although the effect of separation distance on the vibration behavior is noticeable, its effect diminishes for a constant average radius. Therefore, for designing a spiral cylinder, it is appropriate to select the geometrical parameters of equivalent circular cylinder at first step. Then, by considering the radius of circular cylinder as average radius of spiral cylinder, various pairs of separation distance and inner radius can be suggested.

Acknowledgment

NMP is supported by the European Research Council PoC 2015 “Silkene” no. 693670, by the European Commission H2020 under the Graphene Flagship Core 1 no. 696656 (WP14 “Polymer Nanocomposites”) and FET Proactive “Neurofibres” grant no. 732344.

Appendix A

Generally, the position vector of a point on the mid-surface of a shell can be defined by two curvilinear coordinates (α, β) in the global Cartesian coordinate system as:

$$\vec{r} = X(\alpha,\beta)\vec{i} + Y(\alpha,\beta)\vec{j} + Z(\alpha,\beta)\vec{k} \tag{A1}$$

One can determine the magnitude of an infinitesimal distance between two points in the mid-surface of the shell by:

$$(ds)^2 = d\vec{r}.d\vec{r} = \frac{\partial\vec{r}}{\partial\alpha}.\frac{\partial\vec{r}}{\partial\alpha}(d\alpha)^2 + 2\frac{\partial\vec{r}}{\partial\alpha}.\frac{\partial\vec{r}}{\partial\beta}d\alpha\,d\beta + \frac{\partial\vec{r}}{\partial\beta}.\frac{\partial\vec{r}}{\partial\beta}(d\beta)^2 \tag{A2}$$

For the orthogonal curvilinear coordinates relation (A2) reduces to:

$$(ds)^2 = d\vec{r}.d\vec{r} = A^2(d\alpha)^2 + B^2(d\beta)^2 \tag{A3}$$

where A and B are the coefficients of fundamental form or Lame parameters and can be expressed as

$$A = \left|\frac{\partial\vec{r}}{\partial\alpha}\right|; \quad B = \left|\frac{\partial\vec{r}}{\partial\beta}\right| \tag{A4}$$

In fact, the Lame parameters relate the change in curvilinear coordinates to change in arc length. The principle radii of curvatures for two curvilinear coordinate lines can be determined as

$$R_\alpha = \frac{A^2}{\hat{n}.\frac{\partial^2\vec{r}}{\partial\alpha^2}}; \quad R_\beta = \frac{B^2}{\hat{n}.\frac{\partial^2\vec{r}}{\partial\beta^2}} \tag{A5}$$

Where $\hat{n}$ represents the unit vector normal to the surface and is calculated using following equation:

$$\hat{n} = \frac{\frac{\partial\vec{r}}{\partial\alpha}}{A} \times \frac{\frac{\partial\vec{r}}{\partial\beta}}{B} \tag{A6}$$

Appendix B

In this appendix a detailed expressions of generalized stiffness and mass matrices are presented. The following relations can be used to determine each element in submatrices of generalized stiffness and mass matrices.

$$\begin{aligned}
(k_{uu})_{ij} &= A_{11}II^{11}I_1^{00} + A_{66}II^{00}I_{-1}^{11} + k_u^{x_0}(-1)^{m+p}I_1^{00} \\
&\quad + k_u^{x_L}I_1^{00} + k_u^{\theta_0}(-1)^{n+q}II^{00} + k_u^{\theta_\phi}II^{00} \\
(k_{uv})_{ij} &= A_{12}II^{10}I_0^{01} + A_{66}II^{01}I_0^{10} \\
(k_{uw})_{ij} &= A_{12}II^{10}I_0^{00} \\
(k_{vv})_{ij} &= A_{22}II^{00}I_{-1}^{11} + A_{66}II^{11}I_1^{00} + D_{22}II^{00}I_{-3}^{11} \\
&\quad - aD_{22}II^{00}I_{-4}^{01} - aD_{22}II^{00}I_{-4}^{10} + a^2D_{22}II^{00}I_{-5}^{00} \\
&\quad + D_{66}II^{11}I_{-1}^{00} + k_v^{x_0}(-1)^{m+p}I_1^{00} + k_v^{x_L}I_1^{00} \\
&\quad + k_v^{\theta_0}(-1)^{n+q}II^{00} + k_v^{\theta_\phi}II^{00} \\
(k_{ww})_{ij} &= A_{22}II^{00}I_{-1}^{00} + D_{11}II^{22}I_1^{00} - aD_{12}II^{20}I_{-2}^{01} \\
&\quad + D_{12}II^{20}I_{-1}^{02} - aD_{12}II^{02}I_{-2}^{10} + D_{12}II^{02}I_{-1}^{20} \\
&\quad + a^2D_{22}II^{00}I_{-5}^{11} - aD_{22}II^{00}I_{-4}^{12} - aD_{22}II^{00}I_{-4}^{21} \\
&\quad + D_{22}II^{00}I_{-3}^{22} + 4D_{66}II^{11}I_{-1}^{11} + k_w^{x_0}(-1)^{m+p}I_1^{00} \\
&\quad + k_w^{x_L}I_1^{00} + k_w^{\theta_0}(-1)^{n+q}II^{00} + k_w^{\theta_\phi}II^{00} \\
&\quad + \frac{4}{L^2}k_T^{x_0}m^2p^2(-1)^{m+p}I_1^{00} + \frac{4}{L^2}k_T^{x_L}m^2p^2I_1^{00} \\
&\quad + \frac{4}{{\theta_0}^2}k_T^{\theta_0}n^2q^2(-1)^{n+q}II^{00} + \frac{4}{{\theta_0}^2}k_T^{\theta_\phi}n^2q^2II^{00} \\
(M_{uu})_{ij} &= (M_{vv})_{ij} = (M_{ww})_{ij} = \rho hII^{00}I_1^{00}
\end{aligned} \tag{B1}$$

where i and j are defined indexes based on unknown coefficients of displacements $i = m(N+1)+n+1$ and $j = p(N+1)+q+1$. The Other parameters could be defined as:

$$\begin{aligned}
II^{ab} &= \int_0^L \frac{d^aP_m(x)}{dx^a}\frac{d^bP_p(x)}{dx^b}dx \\
I_c^{ab} &= \int_0^\phi \frac{d^aP_n(\theta)}{d\theta^a}\frac{d^bP_q(\theta)}{d\theta^b}.(R_0 + a\theta)^c d\theta \\
A_{11} &= A_{22} = \frac{E\,h}{1-\nu^2}; \quad A_{12} = \frac{\nu\,E\,h}{1-\nu^2}; \quad A_{66} = \frac{E\,h}{2(1+\nu)} \\
D_{11} &= D_{22} = \frac{E\,h^3}{12(1-\nu^2)}; \quad D_{12} = \frac{\nu\,E\,h^3}{12(1-\nu^2)}; \quad D_{66} = \frac{E\,h^3}{24(1+\nu)}
\end{aligned} \tag{B2}$$

References

[1] Boyd D, Kurt C. Free vibrations of noncircular cylindrical shell segments. AIAA J 1971;9:239–44.
[2] Tang D, Wu G, Yao X, Wang C. Free vibration analysis of circular cylindrical shells with arbitrary boundary conditions by the method of Reverberation-Ray matrix. Shock Vibration 2016;2016 Article ID 3814693, 18 pages.
[3] Wang Q, Shi D, Pang F, Ahad FE. Benchmark solution for free vibration of thick open cylindrical shells on Pasternak foundation with general boundary conditions. Meccanica 2017;52:457–82.
[4] Shi D, Zhao Y, Wang Q, Teng X, Pang F. A unified spectro-geometric-Ritz method for vibration analysis of open and closed shells with arbitrary boundary conditions. Shock Vibration 2016;2016 Article ID 4097123, 30 pages.

[5] Cammalleri M, Costanza A. A closed-form solution for natural frequencies of thin-walled cylinders with clamped edges. Int J Mech Sci 2016;110:116–26.
[6] Semenyuk N, Babich IY, Zhukova N. Natural vibrations of corrugated cylindrical shells. Int Appl Mech 2005;41:512–19.
[7] Ma X, Jin G, Xiong Y, Liu Z. Free and forced vibration analysis of coupled conical–cylindrical shells with arbitrary boundary conditions. Int J Mech Sci 2014;88:122–37.
[8] Xing Y, Liu B, Xu T. Exact solutions for free vibration of circular cylindrical shells with classical boundary conditions. Int J Mech Sci 2013;75:178–88.
[9] Zhang L, Xiang Y. Exact solutions for vibration of stepped circular cylindrical shells. J Sound Vibration 2007;299:948–64.
[10] Khalifa AM. Exact solutions for the vibration of circumferentially stepped orthotropic circular cylindrical shells. Comptes Rendus Mecanique 2011;339:708–18.
[11] Dai L, Yang T, Du J, Li W, Brennan M. An exact series solution for the vibration analysis of cylindrical shells with arbitrary boundary conditions. Appl Acoustics 2013;74:440–9.
[12] Chen Y, Jin G, Liu Z. Free vibration analysis of circular cylindrical shell with non-uniform elastic boundary constraints. Int J Mech Sci 2013;74:120–32.
[13] Qu Y, Hua H, Meng G. A domain decomposition approach for vibration analysis of isotropic and composite cylindrical shells with arbitrary boundaries. Composite Struct 2013;95:307–21.
[14] Xie X, Zheng H, Jin G. Integrated orthogonal polynomials based spectral collocation method for vibration analysis of coupled laminated shell structures. Int J Mech Sci 2015;98:132–43.
[15] Selmane A, Lakis AA. Dynamic analysis of anisotropic open cylindrical shells. Comput Struct 1997;62:1–12.
[16] Zhang L, Xiang Y. Vibration of open cylindrical shells with stepped thickness variations. J Eng Mech 2006;132:780–4.
[17] Abbas LK, Lei M, Rui X. Natural vibrations of open-variable thickness circular cylindrical shells in high temperature field. J Aerosp Eng 2009;23:205–12.
[18] Ye T, Jin G, Chen Y, Shi S. A unified formulation for vibration analysis of open shells with arbitrary boundary conditions. Int J Mech Sci 2014;81:42–59.
[19] Ataabadi PB, Khedmati MR, Ataabadi MB. Free vibration analysis of orthtropic thin cylindrical shells with variable thickness by using spline functions. Latin Am J Solids Struct 2014;11:2099–121.
[20] Yamada G, Irie T, Tagawa Y. Free vibration of non-circular cylindrical shells with variable circumferential profile. J Sound Vibration 1984;95:117–26.
[21] Suzuki K, Shikanai G, Leissa A. Free vibrations of laminated composite non-circular thick cylindrical shells. Int J Solids Struct 1996;33:4079–100.
[22] Suzuki K, Shikanai G, Leissa A. Free vibrations of laminated composite noncircular thin cylindrical shells. J Appl Mech 1994;61:861–71.
[23] Ahmed MK. A new vibration approach of an elastic oval cylindrical shell with varying circumferential thickness. J Vibration Control 2011;18(1):117–31.
[24] Hayek SI, Boisvert JE. Vibration of elliptic cylindrical shells: higher order shell theory. J Acoustical Soc Am 2010;128:1063–72.
[25] Lo H-C, Hyer MW. Fundamental natural frequencies of thin-walled elliptical composite cylinders. J Composite Mater 2012;46:1169–90.
[26] Khalifa M. Effects of non-uniform Winkler foundation and non-homogeneity on the free vibration of an orthotropic elliptical cylindrical shell. Eur J Mech-A/Solids 2015;49:570–81.
[27] Soldatos KP. Mechanics of cylindrical shells with non-circular cross-section: a survey. Appl Mech Rev 1999;52:237–74.
[28] Srinivasan R, Bobby W. Free vibration of non-circular cylindrical shell panels. J Sound Vibration 1976;46:43–9.
[29] Massalas C, Soldatos K, Tzivanidis G. Free vibrations of non-circular cylindrical panels with arbitrary boundary conditions. J Sound Vibration 1980;69:491–5.
[30] Koumousis V, Armenakas A. Free vibration of noncircular cylindrical panels with simply supported curved edges. J Eng Mech 1984;110:810–27.
[31] Koumousis VK, Armenàkas AE. Free vibrations of oval cylindrical panels. J Eng Mech 1984;110:1107–23.
[32] Suzuki K, Leissa A. Exact solutions for the free vibrations of open cylindrical shells with circumferentially varying curvature and thickness. J Sound Vibration 1986;107:1–15.
[33] Koumousis V. An explicit method for the free vibrations of non-circular cylindrical panels. J Sound Vibration 1996;191:681–94.
[34] Grigorenko AY, Puzyrev S, Volchek E. Investigation of free vibrations of noncircular cylindrical shells by the spline-collocation method. J Math Sci 2012;185:824–36.
[35] Ventsel E, Krauthammer T. Thin plates and shells: theory: analysis, and applications. CRC Press; 2001.
[36] Shi X, Pugno NM, Cheng Y, Gao H. Gigahertz breathing oscillators based on carbon nanoscrolls. Appl Phys Lett 2009;95:163113.
[37] Cheng Y, Shi X, Pugno NM, Gao H. Substrate-supported carbon nanoscroll oscillator. Phys E 2012;44:955–9.
[38] Shi X, Cheng Y, Pugno NM, Gao H. A translational nanoactuator based on carbon nanoscrolls on substrates. Appl Phys Lett 2010;96:053115.
[39] Taraghi Osgui A, Ahmadian MT, Asghari M, Pugno NM. A shell model for free vibration analysis of carbon nanoscroll. Materials 2017;10:387.
[40] Ye T, Jin G, Shi S, Ma X. Three-dimensional free vibration analysis of thick cylindrical shells with general end conditions and resting on elastic foundations. Int J Mech Sci 2014;84:120–37.
[41] Ye T, Jin G, Su Z, Jia X. A unified Chebyshev–Ritz formulation for vibration analysis of composite laminated deep open shells with arbitrary boundary conditions. Arch Appl Mech 2014;84:441–71.